Journal of Solid State Chemistry **166,** 182–190 (2002)
doi:10.1006/jssc.2002.9579, available online at http://www.idealibrary.com on IDEAL®

Crystallization of Sol–Gel Boehmite via Hydrothermal Annealing

X. Bokhimi,*,[1] J. Sánchez-Valente,† and F. Pedraza†

*Institute of Physics, The National University of Mexico (UNAM), A.P. 20-364, 01000 México D.F., Mexico; and †Instituto Mexicano del Petróleo, Eje Central L. Cárdenas 152, A.P. 14-805, 07730 México D.F., Mexico

Received September 5, 2001; in revised form February 28, 2002; accepted March 8, 2002

Thin crystallites of boehmite were synthesized by annealing a sol–gel precursor under hydrothermal conditions. Samples were characterized with X-ray powder diffraction, thermogravimetry, transmission electron microscopy, and by refining the crystalline phases. Fresh samples consisted of boehmite sheets forming folded paper-like "crystallites," which were transformed into thin flat crystalline plates perpendicular to crystallographic *b*-axis when they were annealed under hydrothermal conditions using water as mineralizer. Boehmite's crystallite size increased with the annealing time. The rhombic boehmite crystallites had their shortest diagonal parallel to crystallographic *a*-axis, and their lateral faces parallel to {101} planes forming an angle of 104.32° between each other; these planes contained active aluminum atoms responsible for the crystallites growing along them. The hydrogen bonding length, which decreased as crystallite size increased, determined the variation of boehmite's transition temperature into γ-alumina. Since this transformation is pseudo-morphic, both particle morphology and sample porosity of alumina were determined by the arrangement of crystallites in boehmite. γ-Alumina crystallite distribution had memory about boehmite crystallite dimensions and atomic arrangement: crystallites were oriented parallel to boehmite's *a* axis, and were confined by boehmite's crystallite dimensions.

Key Words: **sol–gel boehmite; hydrothermal treatment; X-ray powder diffraction; boehmite's crystallite orientation; γ-alumina particle morphology; alumina precursor.**

INTRODUCTION

Among metal oxides, alumina is the most common catalyst and catalyst support used in heterogeneous catalysis; because of its low cost, good thermal stability, high specific surface area, surface acidity and its interaction with deposited transition metals (1–4). Precipitation, drying and calcination of aluminum oxy-hydroxides are the most usual methods to produce it in industry. Aluminas applications require that their precursor hydroxides be free of impurities, like sodium or iron (5).

To understand the evolution of the alumina catalytic properties, it is necessary to prepare catalysts with well-known structure and texture. In this way, a great effort has been carried out for controlling the crystalline structure of the alumina (4, 6), as well as its surface properties; for example, by changing the synthesis conditions (7). These properties can vary with the alumina hydration degree or the impurities incorporated into its crystalline structure.

From the synthesis methods, the sol–gel one allows the control of the textural and structural properties of the solid: the specific surface area, pore size and solid purity. Despite the efforts for using the sol–gel technique to prepare materials of catalytic interest, they are not yet as mature as those obtained for glasses and ceramics (8–11).

Several papers claim that the only way to obtain mesoporous solids with a high surface area from the sol–gel method is using supercritical or freeze drying (11–18). Recently, different alumina aerogels have been prepared using the supercritical drying technique; the solids had high porosity and different morphology to those obtained by using the common drying (xerogels) (11–18). The main restrictions for using these aerogels are associated with the lack of knowledge about many of their physical and chemical properties; for example, their thermal stability, phase transformations, and morphological changes. When gels are treated thermally, their decomposition and surface properties depend on the structure and morphology of the precursor material (9–21).

Sol–gel alumina has specific surface areas that apparently do not correspond to a porous material; to understand this behavior, it is necessary to analyze carefully the size and shape of their pores. In catalysis, the pore volume of a material determines many of their technological properties, such as bed volume and product retention. Since we are interested in using the sol–gel alumina for catalytic applications, we need to determine its textural properties. To understand the origin of these properties, it is necessary to know many details of the crystallography, crystal and

[1]To whom correspondence should be addressed. Fax: + 525-622-5008. E-mail: bokhimi@fisica.unam.mx.

0022-4596/02 $35.00

particle morphology of the alumina and of its precursor, which is boehmite for the present work.

We are reporting the synthesis of boehmite under hydrothermal conditions with water or ethanol as minerilizer (22); the annealing time of synthesis varied from 1 to 15 days. Samples were characterized with X-ray powder diffraction, thermogravimetry and transmission electron microscopy; their crystalline phases were refined with the Rietveld method.

EXPERIMENTAL

Sample Preparation

Aluminum tri-sec-butoxide (ATB) (Aldrich 97%) was dissolved and refluxed in absolute anhydrous ethyl alcohol (EtOH) (J.T. Baker) for 1 h. The hydrolysis catalyst, 3N chloride acid, was dropped slowly to the solution while stirring and refluxing for 3 h until gelling. The molar ratios of the precursors were: EtOH:ATB, 60:1; HCl:ATB, 0.03:1; and H_2O:ATB, 1:1.

The hydrothermal treatment was performed in two different ways: first, the gel, without adding anything, was put into the vessel of the autoclave and heated at 200°C for 4 days under autogenous pressure. Second, the gel was mixed with distilled water (1:1 in volume), which expanded the gel volume because water molecules incorporated into gel's network; this new gel was put into the autoclave and heated at 200°C under autogenous pressure for 3, 7, and 15 days. After the hydrothermal annealing, the corresponding products were dried overnight at 100°C in air. Then, they were further annealed in air up to 400°C at 2°C/min, and then at 4°C/min until 700°C; at this temperature they were eventually calcined for 4 h to get γ-alumina.

Characterization

X-ray diffraction. X-ray diffraction patterns of the samples packed in a glass holder were recorded at room temperature with Cu$K\alpha$ radiation in a Bruker Advance D-8 diffractometer that had θ–θ configuration and a graphite secondary-beam monochromator. Diffraction intensity was measured between 10° and 110°, with a 2θ step of 0.02° for 8 s per point. Crystalline structures were refined with the Rietveld technique by using FULLPROF98 code (23); peak profiles modeled with pseudo-Voigt functions (24) contained average crystallite size as one of its characteristic parameters (25). Standard deviations, which show the last figure variation of a number, are given in parentheses. When they correspond to refined parameters, their values are not estimates of the probable error in the analysis as a whole, but only of the minimum possible probable errors based on their normal distribution (26).

Thermoanalysis. The weight loss and temperatures associated with the phase transformations were determined by thermogravimetry with a Perkin-Elmer TG-7 apparatus from room temperature up to 1000°C at 10°C/min.

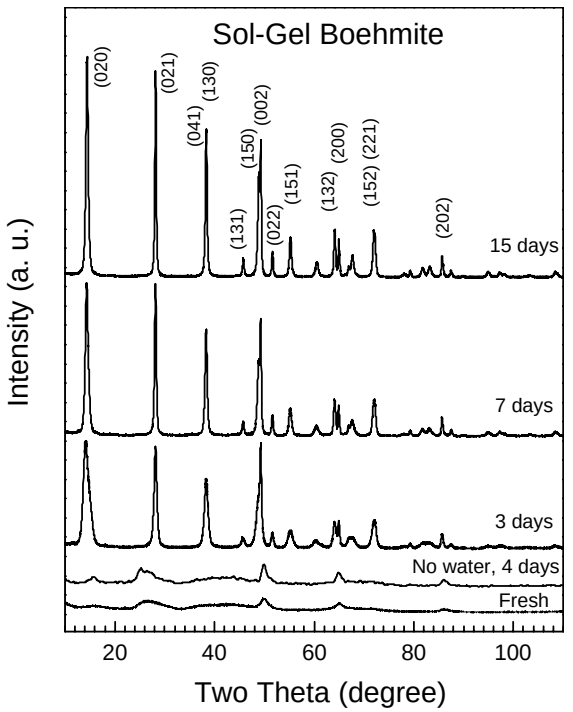

FIG. 1. X-ray diffraction patterns of the boehmite prepared under hydrothermal conditions with water as mineralizer (fresh, and annealed for 3, 7 and 15 days) and without water (4 days). Miller indices correspond to boehmite.

Electron microscopy. The samples milled and dispersed in ethanol before supporting them in the copper grid covered with formvar were observed at 400,000× with in a Jeol 100C× transmission electron microscope that had high-resolution polar pieces.

RESULTS AND DISCUSSION

Crystallization

Crystallization of the gel depended on the mineralizer used for the hydrothermal treatment. When the fresh gel without additional water was placed into the autoclave and annealed at 200°C for 4 days, the samples had nearly the same crystallization as those without the hydrothermal treatment (Fig. 1). The crystallization, however, increased when water was added to the gel before putting it into the autoclave for annealing. The mixture gel–water gave rise to a lighter gel: after adding water the volume of the mixture was much larger than the sum of the separated volumes. When water was added to the gel and formed part of the mineralizer in the hydrothermal treatment, the sample crystallization increased; the crystallite size depended on the

TABLE 1
Boehmite, Space Group *Cmcm*: Atom Fractional Coordinates

Atom	Site	x	y	z
Al	4*c*	0.0	y_{Al}	0.25
O1	4*c*	0.0	y_{O1}	0.25
O2	4*c*	0.0	y_{O2}	0.25

Note. Because X-ray diffraction of hydrogen was negligible, it was not taken into account for the refinement.

TABLE 2
Atom Fractional Coordinates *y*, and Lattice Parameters

Sample	3 days	7 days	15 days
y_{Al}	− 0.3172(1)	− 0.3176(3)	− 0.3176(2)
y_{O1}	0.2902(4)	0.2902(3)	0.2902(2)
y_{O2}	0.0787(4)	0.0778(4)	0.0780(3)
a (nm)	0.28656(2)	0.286676(6)	0.28668(1)
b (nm)	1.2226(2)	1.2223(1)	1.22189(7)
c (nm)	0.36886(3)	0.36907(2)	0.36922(1)

annealing time (for a fixed treatment temperature): crystallites were larger as annealing time increased (Fig. 1).

After the hydrothermal treatment, samples contained only one phase: Boehmite, whose crystalline structure was well modeled with an orthorhombic unit cell having the symmetry described by space group *Cmcm*. To refine this structure, we started with the atom positions given in Table 1 (Table 2 shows the corresponding values after the refinement): O1 corresponded to the sites occupied by the oxygen atoms; O2 to those occupied by the oxygen atoms of hydroxyl groups (Fig. 2).

TEM micrographs showed that boehmite crystals were plates, with dimensions larger along the plate (Fig. 3A) than perpendicular to it (Fig. 3B and Table 3). Since crystal dimensions lay in the nanometric range, the corresponding X-ray diffraction peaks were very broad. Crystallite size alone, however, was insufficient to explain the dependence of the diffraction peak broadening on plane orientation; for example, the broadening caused by planes parallel to crystallite plate faces was larger than expected in comparison with the one produced by the planes perpendicular to these faces. This broadening caused by crystallite dimensions was anisotropic, indicating that they were different. This anisotropy was modeled during refinement using the Rietveld method (Fig. 4).

Crystallite Dimensions

The crystallite dimensions obtained with X-ray diffraction were in good correspondence with those obtained from the TEM micrographs. In the sample annealed for 3 days the average crystallite size, obtained from the refinement, along the *a*-axis, $d_{(200)}$, was 33(2) nm (Table 3), which was similar to many of the crystallite dimensions measured in

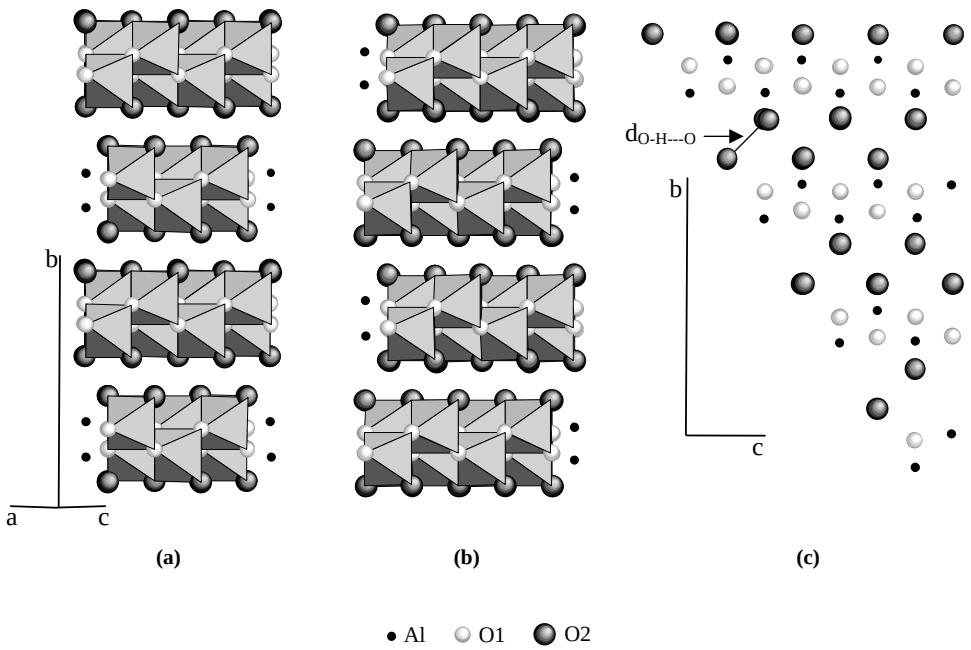

FIG. 2. (A) and (B) Projections of boehmite's crystalline structure on a plane perpendicular to [101] direction; the difference between them is that in (B) the crystallite has grown to the left. (C) Projection of boehmite's crystalline structure on a plane perpendicular to the *a*-axis, and cut by (021) plane; the arrow indicates the hydrogen bonding.

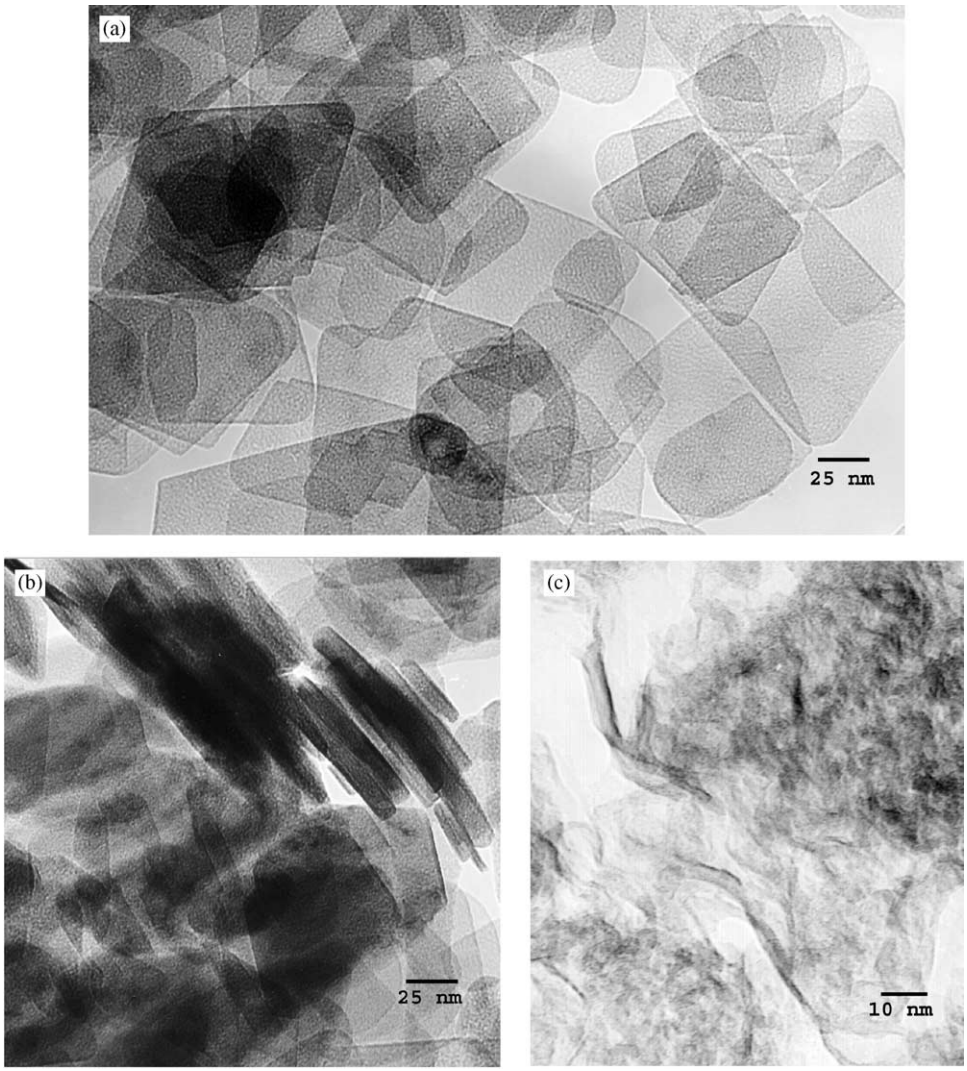

FIG. 3. TEM micrographs of the fresh boehmite sample synthesized for 7 days: (A) The zone axis was parallel to the *b*-axis, (B) lateral view of some crystallites and (C) TEM micrograph of the fresh sol–gel boehmite sample without hydrothermal treatment.

the corresponding micrographs. This correlation was also found for the samples hydrothermally treated for 7 and 15 days. Crystallite dimensions were similar to those obtained when boehmite was precipitated and annealed under the same hydrothermal conditions (27).

The fresh samples of both sol–gel and coprecipitated boehmite, however, had two clear differences. First, the peaks of the diffraction pattern of the fresh precipitated sample were broad but well defined, while in the diffraction pattern of the fresh sol–gel sample, the (020) peak was absent, which is characteristic for boehmite fresh samples (28). This reflects a poor ordering along the *b*-axis (Fig. 2). Second, the (021) reflection for the sol–gel sample shifted to lower diffraction angles (Fig. 1) with respect to its position in the well-crystallized boehmite, in which this peak was at $2\theta = 28.96^\circ$, while it was at 26.62° in the fresh sol–gel sample. Therefore, the distance between (021) planes of the crystallites in the sol–gel sample was larger than in the crystallized sample.

Since (021) planes are related to the hydrogen bonding (Fig. 2C), a larger distance between (021) planes corresponds to a weaker hydrogen bonding and consequently to a lower transition temperature of boehmite into γ-alumina, because this temperature depends on the hydrogen bonding (29). This result is in accordance with the thermogravimetric analysis of the sol–gel samples (Fig. 5), which clearly shows that this transition temperature was much lower for the fresh sample than for those annealed for several days under hydrothermal conditions.

It must be remembered that boehmite crystalline structure is made of layers (perpendicular to the *b*-axis) of octahedra with aluminum atom near its center and oxygen

TABLE 3

Crystallite Dimensions Perpendicular ($d_{(020)}$) and Parallel ($d_{(020)}$) to the Plates, and the Angle δ Between $\{101\}$ Planes as a Function of Synthesis Time. For Comparison, We Give the Corresponding Data for a Coprecipitated Boehmite Annealed Under Hydrothermal Conditions at 180°C (BC180) for 18 h

Sample	$d_{(020)}$ (nm)	$d_{(200)}$ (nm)	δ (deg)
3 days	8.9(1)	33(2)	104.34
7 days	17.6(5)	37(2)	104.32
15 days	22.6(5)	61(4)	104.32
BC180	14.2(2)	43(2)	104.35

and hydroxyls in their vertices (Fig. 2). The layers interact between each other via hydrogen bondings. If this bonding is weak, as in the fresh sol–gel sample, the formation of boehmite's crystalline structure occurs with difficulty, and the layers are almost independent of each other, producing *quasi*-isolated boehmite layers.

The micrograph of the fresh sol–gel sample did not show planar objects; instead, the particles look more like folded sheets (Fig. 3C). This and the fact that the (021) reflection was very broad (additionally to its shifting) suggest that the octahedra building the layer relax to states energetically more stable than the corresponding ones in the planar sheets of well-crystallized boehmite.

The (002), (200) and (202) reflections in the diffraction pattern of the sol–gel fresh sample show that the atoms in the *quasi*-isolated boehmite folded layers were ordered along the dimensions perpendicular to the *b*-axis.

The effect of the hydrothermal treatment was to order these folded layers, building flat plates with a rhombic morphology (Fig. 3A) and average dimensions perpendicular and along the plate that increased with the annealing time (Table 3). The long annealing times show that using the method reported here for the synthesis of boehmite facilitates the control of its crystallite dimensions.

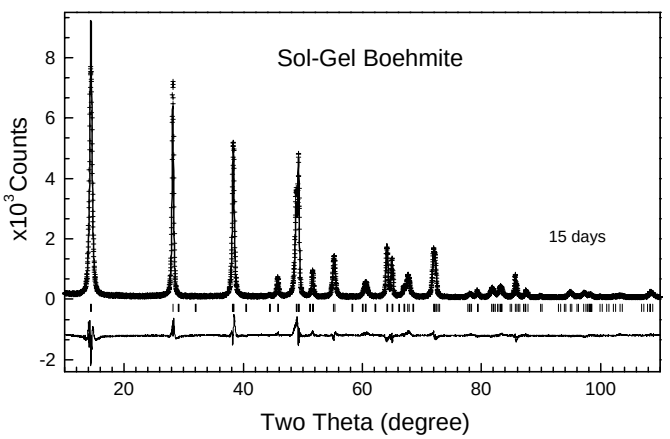

FIG. 4. The Rietveld refinement plot of the boehmite synthesized for 15 days. Crosses correspond to experimental data, continuous lines to the calculated diffraction pattern and the difference between this and the experimental data. Tick marks correspond to boehmite.

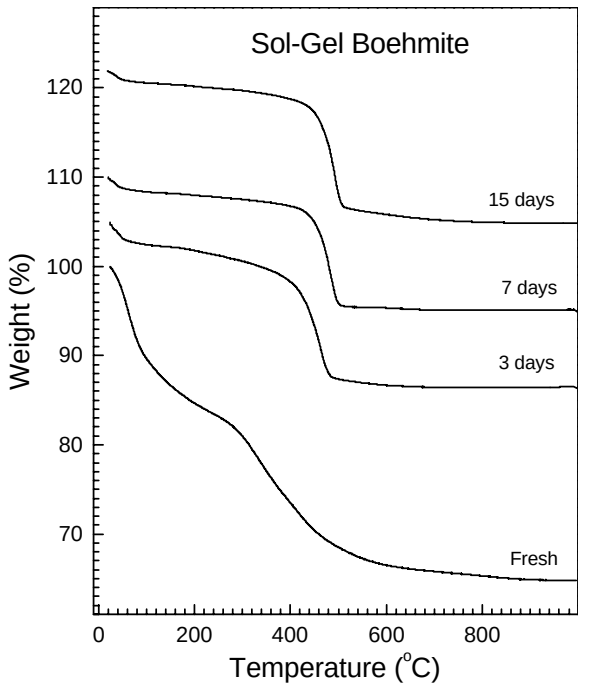

FIG. 5. Thermogravimetric curves of the boehmite samples prepared at different times of hydrothermal treatment.

Crystallite Orientation and Growing

From the micrographs, it is observed that the wider angle, formed by the crystallite faces perpendicular to its face projected on micrographs plane along [020] zone axis (Fig. 3A) was between 104.3° and 110°. If we assume that the lowest angle corresponds to the situation where the crystallite was perpendicular to electron beam, then when a crystallite was not perpendicular to it, the projection of the 104.3 angle on micrograph's plane will give a larger value. Therefore, the measured angles larger than 104.3 came from crystallites that were not perpendicular to [020] zone axis.

When the crystalline structure of boehmite was projected perpendicular to the *b*-axis (Fig. 6), which is the axis perpendicular to crystallite plates, it was observed that the angle δ between $\{101\}$ planes was 104.32° (Table 3). It is the same angle as the one measured in the micrographs for the crystallites. This shows that the crystallite surfaces perpendicular to the plates were parallel to $\{101\}$ planes. Figures 2A and 2B show the structure cut by (101) plane, which cuts the [101] direction (Fig. 6). In these figures, the lateral sides parallel to the *b*-axis are the projection of $(1\bar{0}1)$ planes, which shows clearly that on $\{101\}$ planes aluminum atoms

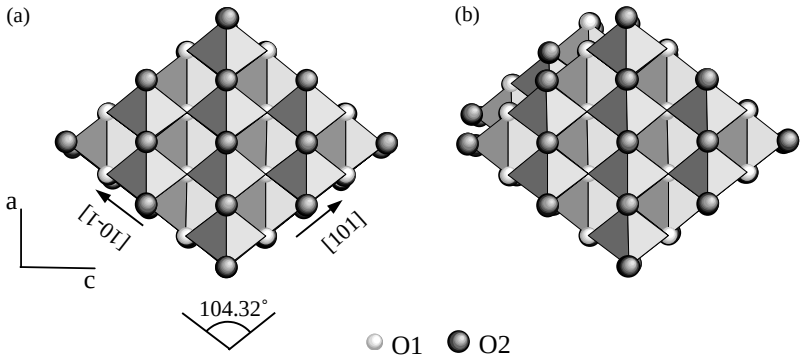

FIG. 6. Projection of boehmite's crystalline structure on a plane perpendicular to *b*-axis. The difference between (A) and (B) is that in (B) the crystallite has grown.

are exposed to the surface. There are two atoms per projection of the unit cell on any $\langle 101 \rangle$ direction (Figs. 2A and 2B); this gives an average of 2924, 6467 and 13,685 aluminum atoms exposed to the surface per crystallite for the samples annealed for 3, 7 and 15 days, respectively. These values correspond to 7.61, 6.76, and $4.11 + 10^{9}$ aluminum atoms per gram of boehmite, respectively.

According to the above analysis, the *a*-axis bisects the measured angle of 104.32° (Fig. 6A) and was parallel to the shorter diagonal in the observed crystallites; then, the larger diagonal was parallel to the *c*-axis.

Since crystallites grew mainly along the $\langle 101 \rangle$ directions, the aluminum atoms on $\{101\}$ planes should be chemically very reactive. All other sites of boehmite crystallite surface are occupied by hydroxyls, whose chemical activity only depends on its capability of forming hydrogen bonds.

When a boehmite's crystallite grows, the active aluminum atoms reacts with oxygen and hydroxyls from the environment, completing its corresponding octahedron (Figs. 2B and 6B), and create holes in the neighboring boehmite layer, which are appropriated for binding other aluminum atoms from the environment. This cyclic mechanism explains the growing process of boehmite crystallites. Since crystallite growing along the *b*-axis is determined by hydrogen bonding, which is much weaker than the interaction of aluminum atoms on the lateral surfaces with its environment, the growth along [010] direction occurred less frequently, and boehmite crystallites grew preferentially perpendicular to the *b*-axis.

TABLE 4
Transition Temperature of Boehmite Into γ-Alumina, and Hydrogen Bonding Length $d_{O-H\cdots O}$ as a Function of Synthesis Time

Sample	*T* (C)	$d_{O-H\cdots O}$ (nm)
3 days	462.0	0.2665(1)
7 days	483.1	0.2650(1)
15 days	491.1	0.2650(1)

Transformation of Boehmite into γ-Alumina

The transformation temperature of boehmite into γ-alumina depended on the time the precursor gel was under hydrothermal conditions (Fig. 5 and Table 4). The fresh sample transformed at a very low temperature; the derivative of its thermogravimetry curve showed two minima: the

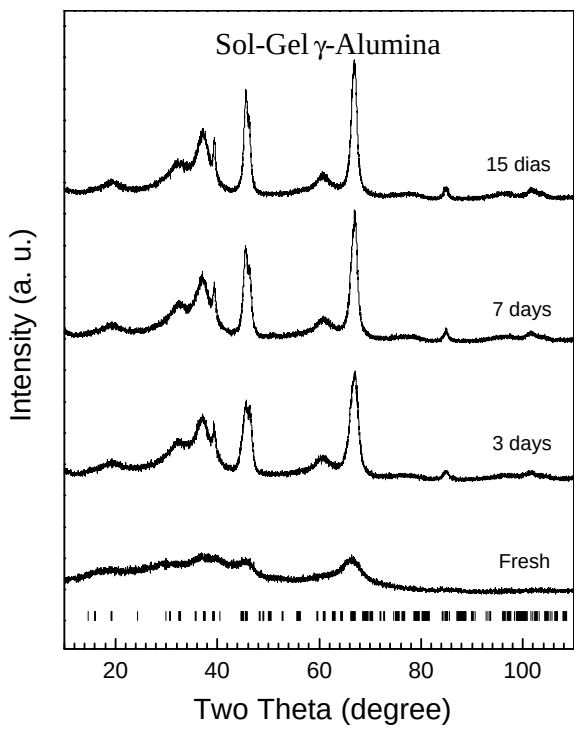

FIG. 7. X-ray diffraction pattern of the γ-alumina samples prepared from boehmite synthesized under hydrothermal conditions for different times.

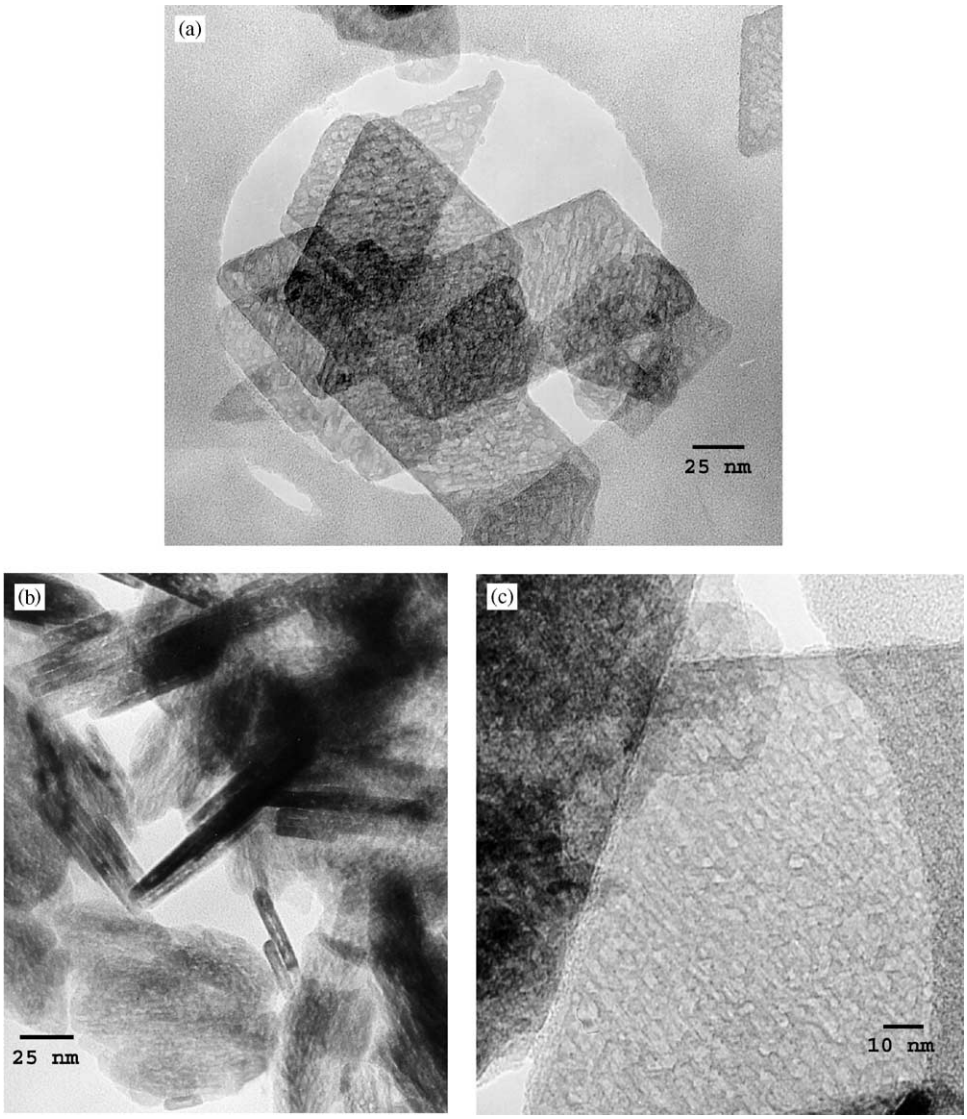

FIG. 8. TEM micrographs of the γ-alumina prepared from boehmite synthesized for 7 days: In (A) the zone axis was parallel to the *b*-axis; (B) shows a lateral view of many γ-alumina particles that were originally single boehmite crystallites and (C) is a TEM micrograph of the γ-alumina prepared from the boehmite synthesized for 15 days; the zone axis was parallel to the *b*-axis.

largest one at 336.3°C and the other at 419.4°C. The presence of two minima points out the non-uniform distribution of crystallite dimensions in this sample. As it was mentioned above, this low transition temperature was due to the weak hydrogen bonding between hydroxyls. The crystallized samples had transition temperatures between 460°C and 500°C (Table 4); the temperature increased with the synthesis annealing time, and correlated well with the corresponding hydrogen bonding lengths (Table 4). As this length decreased, the transformation temperature increased, corroborating the reported dependence of this transition temperature with hydrogen bonding (28). It is worthwhile to note that the hydrogen bonding length of all sol–gel samples was shorter than the values reported for the samples prepared from coprecipitated seeds (28), for which the shortest value was $d_{O-H\cdots O} = 0.2681(1)$ nm. Therefore, the binding between boehmite layers in the sol–gel samples was stronger.

When the samples were heated at 700°C, they transformed into γ-alumina (Figs. 7 and 8) with a crystallite size that depended on the crystallite dimension of the corresponding boehmite (Tables 3 and 5). As in previous studies on boehmite (29, 30), to obtain information about the lattice parameters and average crystallite size of γ-alumina, its structure was refined with a monoclinic unit cell derived from the spinel (31). This model did not fit very well with the

TABLE 5

Lattice Parameters and Average Crystallite Size of the γ-Alumina Derived from Boehmite Precursor Prepared for Different Annealing Times

Precursor	*a* (nm)	*b* (nm)	*c* (nm)	*β* (deg)	*d* (nm)
3 days	1.2106(5)	0.2800(1)	0.5561(2)	103.11(3)	4.9(1)
7 days	1.2129(3)	0.2799(1)	0.5565(2)	102.97(3)	5.9(1)
15 days	1.2143(4)	0.2798(1)	0.5576(2)	103.04(3)	6.4(4)

structure of this phase, but helped to get information about it; the results are better than those obtained with a cubic or tetragonal structure. Crystallite size as obtained after the refinement were 4.9(1), 5.9(1), and 6.4(4) nm for the samples annealed for 3, 5 and 15 days, respectively. These sizes were notoriously shorter than the dimensions of the boehmite's crystallite size along the faces perpendicular to the *b*-axis (Table 3).

The thin boehmite crystallites were transformed into thin laminar polycrystalline particles of γ-alumina (Fig. 8). This morphology was responsible of the porosity in the sample. Since the transformation of boehmite into γ-alumina is pseudo-morphic, the alumina particles also maintained the morphology of the original boehmite crystallites along the plates (Figs. 8A and 8B).

γ-Alumina crystallites had memory of boehmite crystallites orientation (Fig. 8C). Alumina crystallites were not oriented at random. From a careful analysis of alumina micrographs, it was observed that in an alumina particle, which basically corresponded to a boehmite single crystallite, alumina crystallites were oriented along the *a*-axis of the boehmite precursor, which is parallel to the shortest diagonal of the rhombic crystallites. This direction in the calcined samples corresponded to the shortest diagonal of the rhombic alumina particle.

CONCLUSIONS

Sol–gel boehmite crystallized when it was annealed under hydrothermal conditions with water as mineralizer; the absence of this solvent inhibited crystal growing. Boehmite's crystallite dimensions grew with the annealing time. The sol–gel samples without hydrothermal treatment consisted of folded paper-like boehmite "crystallites," characterized by a weak hydrogen bonding, which were transformed into thin flat crystalline plates perpendicular to the *b*-axis when they were annealed under hydrothermal conditions. Boehmite crystallite plates were rhombic with its shortest diagonal parallel to the *a*-axis; their lateral faces were parallel to {101} planes, forming an angle of 104.32° and containing active aluminum atoms on them, which were responsible for crystallite growing along these faces. Hydrogen bonding length decreased as crystallite size increased, and determined the variation of the transition temperature of boehmite into γ-alumina. Since this transformation is pseudomorphic, the particle morphology and the sample porosity of alumina were determined by the arrangement of crystallites in boehmite. γ-Alumina crystallite distribution had memory about boehmite crystallite dimensions and atomic arrangement; they were oriented parallel to boehmite's *a*-axis, and were confined by boehmite crystallite dimensions.

ACKNOWLEDGMENTS

We thank Mr. A. Morales and Mr. M. Aguilar for technical assistance. This work was financially supported by the project D.01024 under the IMP-Maya Crude Oil Research Program.

REFERENCES

1. T. Kotanigawa, M. Yamamoto, M. Utiyama, H. Hattori, and K. Tanabe, *Appl. Catal.* **1,** 185 (1981).
2. K. Hellgardt and D. Chadwick, *Ind. Eng. Chem. Res.* **37,** 405 (1998).
3. B. Beguin, E. Garboswki, and M. Primet, *J. Catal.* **127,** 595 (1991).
4. H. Knözinger and P. Ratnasamy, *Catal Rev.—Sci. Eng.* **17,** 31 (1978).
5. F. Vaudry, S. Khodabandeh, and M. E. Davis, *Chem. Mater.* **8,** 1451 (1996).
6. B. C. Lippens, "Structure and Texture of Aluminas," Thesis, Uitgeverij Waltman, Delft, 1961.
7. K. Jiratova and L. Beranek, *Appl. Catal.* **2,** 125 (1982).
8. D. A. Ward and E. I. Ko, *I&EC Res.* **34,** 421 (1995).
9. S. J. Monaco and E. I. Ko, *Chem. Mater.* **9,** 2404 (1997).
10. J. Livage, *Catal. Today* **4,** 3 (1998).
11. A. C. Pierre, E. Elaloui, and G.M. Pajonk, *Langmuir* **14,** 66 (1998).
12. J. N. Armor and E. J. Carlson, *J. Mater. Sci.* **22,** 2549 (1987).
13. A. J. Fanelli, S. Verma, T. Engelmann, and J. V. Burlew, *Ind. Eng. Chem. Res.* **30,** 126 (1991).
14. J. S. Dong and P. Tae-Jin, *Chem. Mater.* **9,** 1903 (1997).
15. S. Keysar, G. E. Shter, Y. deHazan, Y. Cohen, and G. S. Grader, *Chem. Mater.* **9,** 2464 (1997).
16. G. M. Pajonk, *Catal. Today* **35,** 319 (1997).
17. Y. Mizushima and M. Hori, *J. Non-Cryst. Solids* **167,** 1 (1994).
18. M. Schneider and A. Baiker, *Catal. Rev.—Sci. Eng.* **37,** 515 (1995).
19. B. E. Yoldas, *J. Mater. Sci.* **10,** 1856 (1975).
20. J. A. Wang, X. Bokhimi, O. Novaro, T. Lopez, F. Tzompantzi, R. Gomez, J. Navarrete, M. E. Llanos, and E. Lopez-Salinas, *J. Mol. Catal A* **137,** 239 (1999).
21. J. A. Wang, X. Bokhimi, A. Morales, O. Novaro, T. Lopez, and R. Gomez, *J. Phys. Chem. B* **103,** 299 (1999).
22. L. N. Dem'yanets and A. N. Lobachev, *in* "Crystallization Process under Hydrothermal Conditions" (A. N. Lobachev and G. D. Archard, Eds.), p. 1. Consultants Bureu, A Division of Plenum Publishing Coorporation, New York, 1973.
23. J. Rodríguez-Carbajal, "Laboratoire Leon Brillouin (CEA-CNRS)," France.
24. P. Thompson, D. E. Cox, and J. B. Hasting, *J. Appl. Crystallogr.* **20,** 79 (1987).
25. R. A. Young and P. Desai, *Arch. Nauki Mater.* **10,** 71 (1989).
26. E. Prince, *J. Appl. Crystallogr.* **14,** 157 (1981).
27. X. Bokhimi, J. A. Toledo-Antonio, M. L. Guzmán-Castillo, and F. Hernández-Beltrán, *J. Sol. State Chem.* **159,** 32 (2001).

28. A. Vázquez, T. López, R. Gómez, and X. Bokhimi, *J. Mol. Catal. A* **167,** 91 (2001).
29. X. Bokhimi, J. A. Toledo-Antonio, M. L. Guzman-Castillo, B. Mar-Mar, F. Hernández-Beltrán, and J. Navarrete, *J. Solid State Chem.* **161,** 319 (2001).
30. M. L. Guzmán-Castillo, X. Bokhimi, J. Salmones-Blázquez, A. Toledo-Antonio, and F. Hernández-Beltrán, *J. Phys. Chem. B* **105,** 2099 (2001).
31. E. Husson and Y. Repelin, *Eur. J. Solid State Inorg. Chem.* **33,** 1223 (1996).